Proc. Natl. Acad. Sci. USA
Vol. 90, pp. 9678–9682, October 1993
Neurobiology

Synthetic peptides homologous to prion protein residues 106–147 form amyloid-like fibrils *in vitro*

FABRIZIO TAGLIAVINI*†, FRANCES PRELLI‡, LAURA VERGA*, GIORGIO GIACCONE*, RAGUPATHY SARMA§, PETER GOREVIC¶, BERNARDINO GHETTI‖, FLAVIO PASSERINI**, ELENA GHIBAUDI**, GIANLUIGI FORLONI**, MARIO SALMONA**, ORSO BUGIANI*, AND BLAS FRANGIONE‡

*Istituto Nazionale Neurologico Carlo Besta, 20133 Milan, Italy; ‡Department of Pathology, New York University Medical Center, New York, NY 10016; Departments of §Biochemistry and ¶Medicine, State University of New York, Stony Brook, NY 11794; ‖Department of Pathology, Indiana University School of Medicine, Indianapolis, IN 46202-5120; and **Istituto di Ricerche Farmacologiche Mario Negri, 20157 Milan, Italy

Communicated by Aaron Klug, June 28, 1993

ABSTRACT **Gerstmann–Sträussler–Scheinker disease (GSS) is a prion-related encephalopathy pathologically characterized by massive deposition of prion protein (PrP) amyloid in the central nervous system. The major component of amyloid fibrils isolated from patients of the Indiana kindred of GSS (GSS-Ik) is an 11-kDa fragment of PrP spanning residues 58 to ≈150. These patients carry a missense mutation of the *PRNP* gene, causing a Phe → Ser substitution at codon 198. We investigated fibrillogenesis *in vitro* by using synthetic peptides homologous to consecutive segments of GSS-Ik amyloid protein (residues 57–64, 89–106, 106–126, and 127–147) as well as peptides from the PrP region with the GSS-Ik mutation (residues 191–205 and 181–205, both wild type and mutant). Peptide PrP-(106–126) formed straight fibrils similar to those extracted from GSS brains, whereas peptide PrP-(127–147) formed twisted fibrils resembling scrapie-associated fibrils isolated from subjects with transmissible spongiform encephalopathies. Congo red staining and x-ray fibril diffraction showed that both straight and twisted fibrils had tinctorial and conformational properties of native amyloid. Conversely, the other peptides did not form amyloid-like fibrils under similar conditions. These findings suggest that the sequence spanning residues 106–147 of PrP is central to amyloid fibril formation in GSS and related encephalopathies.**

The cellular prion protein (PrP^C) is a 33- to 35-kDa sialoglycoprotein expressed in neurons and, to a lesser extent, in other cells (1–3). The protein is either bound to the cell surface by a glycosyl phosphatidylinositol anchor (4) or secreted as a soluble derivative (5). Mutations in the *PRNP* gene segregate with hereditary human disorders such as familial Creutzfeldt–Jakob disease, Gerstmann–Sträussler–Scheinker disease (GSS), and fatal familial insomnia (6). A still undefined posttranslational modification of PrP^C leading to formation of an abnormal PrP isoform designated PrP^{Sc} occurs in transmissible spongiform encephalopathies such as scrapie of sheep and goat, spongiform encephalopathy of cattle, and sporadic Creutzfeldt–Jakob disease of humans (6). The presence of PrP^{Sc} in the cerebral tissue is regarded as the molecular marker for both genetic and transmissible prion-related encephalopathies.

A distinctive feature of PrP^{Sc} is a partial resistance to proteinase K digestion under conditions where PrP^C is completely degraded (7–9). In scrapie and related conditions, the protease-resistant core is an N-terminal truncated fragment of PrP^{Sc} spanning residues 90–231; it has a molecular mass of 27–30 kDa and has been designated PrP 27-30 (7–10). In the presence of detergent, PrP 27-30 aggregates into rod-shaped particles having the tinctorial, optical, and ultrastructural properties of amyloid fibrils (11). Conformational analysis by infrared spectroscopy revealed that PrP 27-30 polymers possess a higher content of β-sheet than predicted (12). On this basis, it has been argued that modifications in secondary and tertiary structure may occur with the conversion of PrP^C to PrP^{Sc} that significantly increase its potential for amyloid fibril formation.

Cerebral deposition of PrP amyloid occurs to the highest degree in GSS (13, 14). This is an adult-onset disorder of postural and cognitive functions that is inherited with an autosomal dominant trait and segregates with a mutation at codon 102, 117, 198, or 217 of the *PRNP* gene (6). The biochemical composition of PrP amyloid has been determined thus far only in brain tissue samples obtained from symptomatic members of the Indiana kindred of GSS (GSS-Ik). These patients carry a missense mutation of the *PRNP* gene causing Phe → Ser substitution at codon 198 (15, 16) and have a distinct neuropathologic phenotype characterized by the association of PrP amyloid deposits and neurofibrillary tangles with paired helical filaments (17–19). The major component of amyloid fibrils of GSS-Ik is an 11-kDa fragment of PrP that spans residues 58 to ≈150 (20). In addition, amyloid fractions contain larger PrP fragments with apparently intact N termini and a lower molecular mass fragment (20). Thus, the main amyloid component in GSS-Ik does not include the region containing the amino acid substitution, although the presence of the mutant residue in other amyloid fractions has not been ruled out. In this regard, the coexistence of PrP amyloid and PrP fragments spanning the mutant Ser-198 has been hypothesized on the basis of immunohistochemical analyses of GSS-Ik brains (21).

These data suggest that much of PrP 27-30 is not required for amyloid fibril formation and raise questions as to the role of point mutations in PrP amyloidogenesis. The present study was undertaken to determine which PrP residues are important for polymerization of PrP peptides into amyloid fibrils and to investigate the relation of the Phe → Ser substitution at PrP codon 198 to fibrillogenesis in this disorder. The analysis utilized synthetic peptides homologous to different fragments of the amyloid protein of GSS-Ik and peptides from the PrP region carrying the GSS-Ik mutation (Fig. 1*a*).

MATERIALS AND METHODS

Synthesis and Purification of Peptides. The peptides for investigation were selected on the basis of the predicted secondary structure (22, 24) and the hydropathic profile (23) of human PrP. By the analysis of these structural parameters,

The publication costs of this article were defrayed in part by page charge payment. This article must therefore be hereby marked "*advertisement*" in accordance with 18 U.S.C. §1734 solely to indicate this fact.

Abbreviations: GSS, Gerstmann–Sträussler–Scheinker disease; GSS-Ik, Indiana kindred of GSS; PrP, prion protein.

†To whom reprint requests should be addressed at: Istituto Nazionale Neurologico Carlo Besta, via Celoria 11, 20133 Milan, Italy.

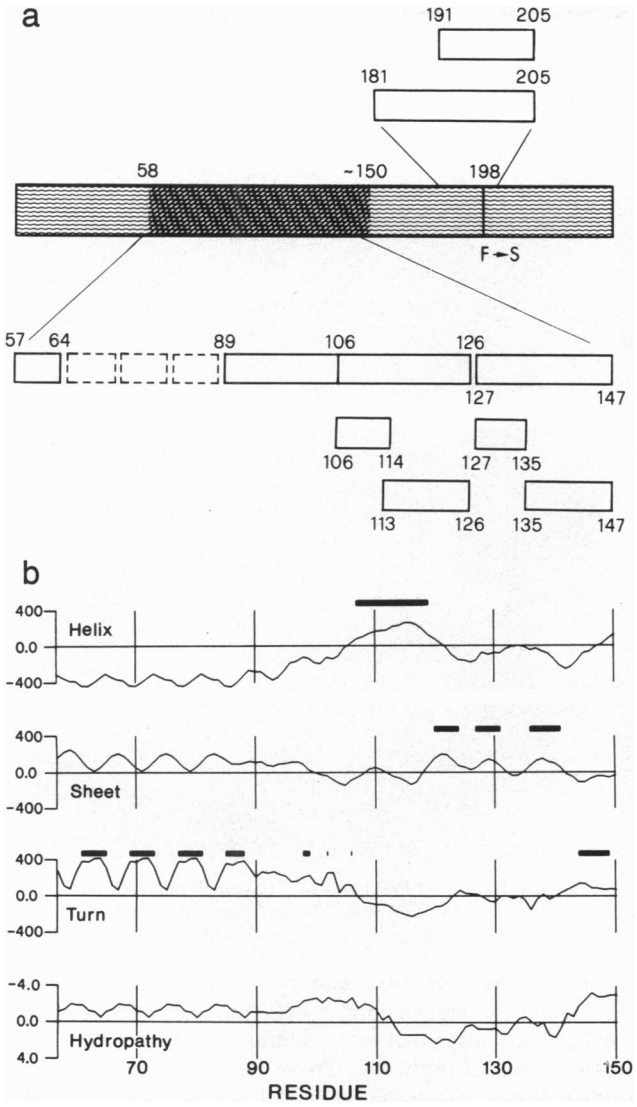

FIG. 1. (*a*) Schematic representation of the PrP molecule indicating the amyloid protein isolated from GSS-Ik brains (darkly shaded area) and of synthetic peptides used in this study. Codon numbers are given for the first and last residue of peptides and for the amino acid substitution site linked to GSS-Ik. (*b*) Predicted secondary structure (22) and hydropathic profile (23) of the PrP region corresponding to the GSS-Ik amyloid protein. Bars indicate high potential sites for α-helix, β-sheet, and β-turn.

the 11-kDa amyloid protein of GSS-Ik was divided in four peptides, corresponding to residues 57–64 (WGQPHGGG), 89–106 (WGQGGGTHSQWNKPSKPK), 106–126 (KTNMKHMAGAAAAGAVVGGLG), and 127–147 (GYMLGSAMSRPIIHFGSDYED) of the amino acid sequence deduced from human PrP cDNA. Peptides PrP-(57–64) (i.e., the octapeptide repeat) and PrP-(89–106) (i.e., the N-terminal region of PrP 27-30) are hydrophilic, whereas PrP-(106–126) and PrP-(127–147) contain a sequence of hydrophobic amino acids flanked by hydrophilic residues at the N terminus and C terminus, respectively. The conformation indices for α-helix, β-sheet, and β-turn of the PrP region containing these peptides are shown in Fig. 1*b*. To further define amino acid sequences critical for fibrillogenesis, peptides PrP-(106–126) and PrP-(127–147) were divided in shorter segments, homologous to residues 106–114 (KTNMKHMAG), 113–126 (AGAAAAGAVVGGLG), 127–135 (GYMLGSAMS), and 135–147 (SRPIIHFGSDYED). Peptides corresponding to residues 191–205 (TTTKGENFTETDVKM) and 181–205 (NITIKQHTVTTTTKGENFTETDVKM) as well as analogues carrying Phe → Ser substitution at residue 198 were synthesized, to evaluate whether the mutation linked to GSS-Ik enhances the inherent fibrillogenic ability of PrP peptides. PrP-(191–205) is hydrophilic and its C-terminal half shows high potential for an α-helix. PrP-(181–205) contains a short sequence of hydrophobic amino acids in front of a long hydrophilic stretch, whose proximal region has high potential for β-sheet formation.

Stepwise solid-phase peptide synthesis was carried out on a model 430A synthesizer (Applied Biosystems), using 9-fluorenylmethoxycarbonyl as the protective group for aminic residues, and *N*-hydroxybenzotriazole, *O*-benzotriazol-1-yl-*N*,*N*,*N*′,*N*′-tetramethyluronium hexafluorophosphate, and *N*,*N*′-dicyclohexylcarbodiimide as activators of carboxylic residues. The peptides were purified by reverse-phase HPLC. Peptides PrP-(113–126) and PrP-(135–147) were obtained by chemical cleavage of PrP-(106–126) and PrP-(127–147) with cyanogen bromide and were purified by reverse-phase HPLC. Identity and purity of all peptides were determined by amino acid analysis using a Beckman model 6300 analyzer (Beckman) and amino acid sequencing by automated Edman degradation with a Milligen model 6600 prosequencer (Millipore). Purity was >95% for all peptides used.

Morphology and Staining Properties of Peptide Assemblies. Because of insolubility of some peptides under physiological conditions, all peptides were dissolved in 30% (vol/vol) formic acid or in 1,1,1,3,3,3-hexafluoro-2-propanol at concentrations of 0.5, 1, 2.5, 5, and 10 mg/ml. The solutions were dialyzed for 24 hr at room temperature against distilled water, or 20 mM citrate buffer (pH 5.5), or phosphate-buffered saline (PBS; pH 7.4). For light microscopy, 50 μl of each suspension was air-dried on gelatin-coated slides, stained with 0.2% congo red in 80% ethanol saturated with NaCl, and examined under polarized light, or treated with 1% aqueous thioflavine S and observed with fluorescent light. For electron microscopy, 5 μl of each suspension was applied to Formvar-coated nickel grids, negatively stained with 5% (wt/vol) uranyl acetate, and observed in an electron microscope model 410 (Philips Electronic Instruments, Mahwah, NJ) at 80 kV.

X-Ray Diffraction Analysis. X-ray diffraction studies were performed on peptides that proved to be fibrillogenic at electron microscopic examination. Peptides were analyzed as a lyophilized powder, allowed to sediment by slow dehydration after suspension in distilled water, or solubilized in either 30% formic acid or 1,1,1,3,3,3-hexafluoro-2-propanol prior to placement into 0.8-mm-diameter siliconized Lindeman glass capillary tubes. Diffraction patterns were obtained after exposure to nickel-filtered CuKα radiation from a sealed x-ray tube generator source operated at 40 kV and 16 mA, with exposure times of 1–2 hr. Bragg spacings were measured directly on reflex 25 x-ray films (CEA); using a specimen-to-film distance of 7.5 cm (25).

RESULTS

Morphology of Peptide Assemblies. Peptides PrP-(57–64) and PrP-(89–106) were soluble in distilled water, citrate buffer, or PBS and did not form fibrils. Conversely, peptides PrP-(106–126) and PrP-(127–147) were sparingly soluble in aqueous solutions and readily formed fibrils that, at electron microscopic examination, exhibited distinct morphologies. PrP-(106–126) fibrils were straight, unbranched, 4–8 nm in diameter ($\bar{x} \pm$ SD = 5.6 ± 0.9 nm), and 0.1–2.0 μm long (Fig. 2*a*). In most preparations, the fibrils formed dense meshworks without order between units (Fig. 2*b*); however, extensive lateral aggregation with regular parallel arrangement was apparent in suspensions of the peptide in citrate buffer (pH 5.5) (Fig. 2*c*). Removal of 12 residues from the C terminus of PrP-(106–126) to yield peptide PrP-(106–114) did

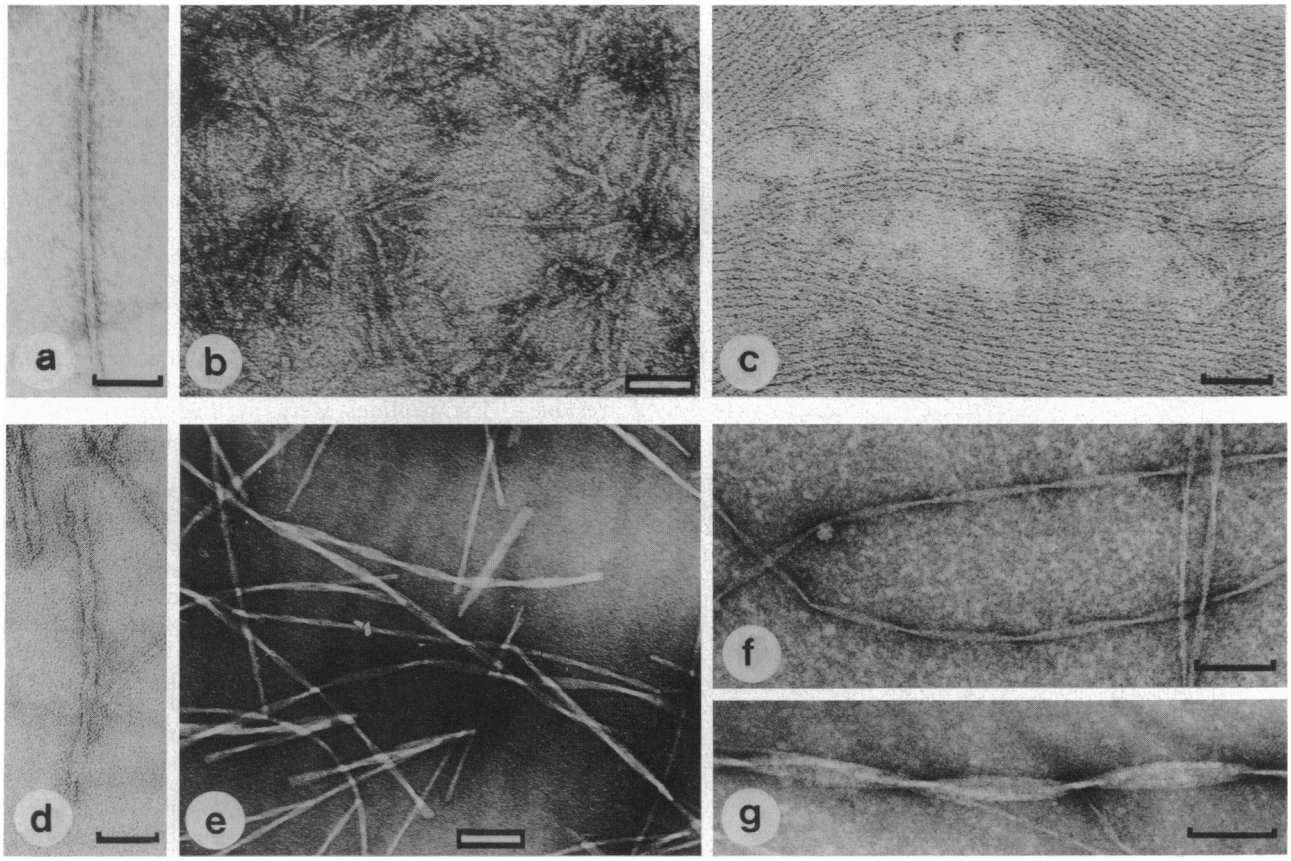

FIG. 2. Electron micrographs of fibrils generated *in vitro* by peptides PrP-(106–126) (*a–c*) and PrP-(127–147) (*d–g*). Peptide PrP-(106–126) formed straight fibrils (*a*) that originated either random meshworks (*b*) or parallel bundles (*c*). Peptide PrP-(127–147) formed straight or twisted fibrils that assembled into helical structures with a periodicity of 60 nm or multiples (*d–g*). (Bars: *a–d*, 50 nm; *e–g*, 100 nm.)

not significantly modify its fibrillogenic ability. PrP-(106–114) was relatively soluble in distilled water, citrate buffer, or PBS and built up a dense network of straight 4- to 8-nm diameter fibrils ($\bar{x} \pm$ SD = 5.4 ± 0.9 nm) morphologically similar to those formed by PrP-(106–126). On the other hand, removal of 7 residues from the N terminus of PrP-(106–126) to yield peptide PrP-(113–126) resulted in noticeable changes in the appearance of fibrils that had a diameter of 3–5 nm ($\bar{x} \pm$ SD = 4.1 ± 0.6 nm) and a length of <0.4 μm. Furthermore, the fibrils were significantly less abundant at equal concentrations of peptide in these preparations.

PrP-(127–147) polymerized into either straight or twisted unbranched fibrils, having a diameter of 5–8 nm ($\bar{x} \pm$ SD = 6.5 ± 1.3 nm) and a length ranging from 0.2 to 3.0 μm. The fibrils showed high tendency to adhere to each other, organizing into bundles of various widths, depending on the number of constituent fibrils (Fig. 2 *d–g*). Coupling of fibrils frequently resulted in the formation of twisted structures with a well-defined pitch. Twisted structures formed by two fibrils showed maximum and minimum widths of ≈16 and ≈8 nm and spacing between crossovers of ≈60 nm (Fig. 2*d*). When these structures were composed of several fibrils, the twists occurred at intervals corresponding to multiples of 60 nm (≈120, ≈180, or ≈240 nm) (Fig. 2 *f* and *g*). PrP-(127–147) fibrillary assemblies were remarkably less compact than those formed by PrP-(106–126) even at peptide concentrations of 5 or 10 mg/ml (Fig. 2*e*); the fibrils were generally observed in disordered array, though on occasion they aggregated into star-like structures. Removal of 12 residues from the C terminus or 8 residues from the N terminus of peptide PrP-(127–147) to yield peptides PrP-(127–135) and PrP-(135–147), resulted in loss of fibrillogenic ability.

Peptides PrP-(191–205) wild type and mutant were not fibrillogenic, whereas peptides PrP-(181–205) exhibited minimal fibril formation that was not influenced by the Phe → Ser substitution at residue 198. These peptides were soluble in distilled water, citrate buffer, and PBS; fibrillar assemblies were only observed at a peptide concentration >5 mg/ml, and the few fibrils that formed were poorly contrasted, short, and straight or slightly curved and had a diameter of 3–4 nm.

Staining Properties of Synthetic Fibrils. Macromolecular assemblies of peptides PrP-(106–126), -(106–114), -(113–126), and -(127–147) exhibited tinctorial and optical properties of *in situ* amyloid—i.e., birefringence under polarized light after congo red staining (Fig. 3 *a* and *b*) and yellow fluorescence after thioflavine S treatment. Congo red binding was stronger for PrP-(106–126), -(106–114), and -(127–147) than for PrP-(113–126). In contrast, the other peptides including PrP-(181–205) wild type and mutant failed to show birefringence or fluorescence.

X-Ray Diffraction Patterns. Lyophilized peptide PrP-(106–126) consisted of small chunky material, which exhibited birefringence by polarizing microscopy. The x-ray pattern from this material showed reflections in the form of two diffuse rings, corresponding to Bragg spacings of 4.48 Å (4.30–4.73 Å) and 3.75 Å (3.70–3.80 Å). This pattern did not change when the capillary tube was rotated by 90°, indicating that the sample was not a single crystal. A more detailed diffraction pattern was obtained when the peptide was suspended in distilled water and allowed to evaporate for 2 days. In addition to the above spacings, the air-dried sample showed two diffuse equatorial reflections, corresponding to Bragg spacings of 5.80 Å (5.60–7.45 Å) and 15.48 Å (10.50–20.10 Å) (Fig. 3*c*). Moreover, the reflections at 4.48 Å and 3.75 Å appeared as

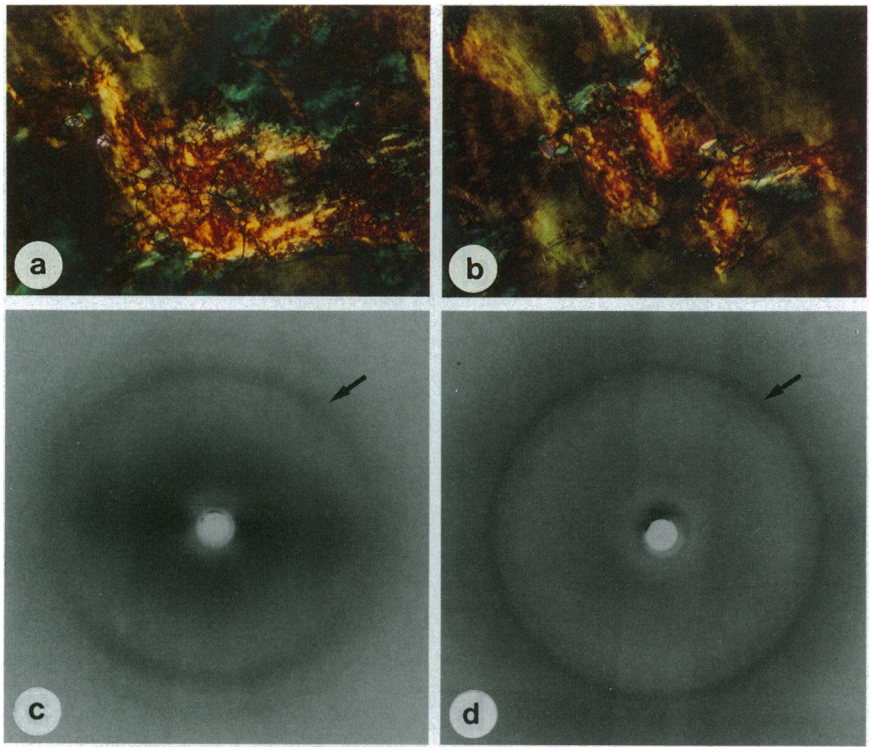

FIG. 3. (*a* and *b*) Birefringence after congo red staining of fibrillary assemblies formed by peptides PrP-(106–126) (*a*) and PrP-(127–147) (*b*), observed through polarized light. (×270.) (*c* and *d*) X-ray diffraction patterns of peptides PrP-(106–126) (*c*) and PrP-(127–147) (*d*) with reflections corresponding to H-bonding between antiparallel β-sheets (arrow). PrP-(106–126) shows two additional equatorial reflections at 5.80 Å (5.60–7.45 Å) and 15.48 Å (10.50–20.10 Å).

large meridional arcs instead of rings, indicating greater order in the specimen.

Hydrated PrP-(106–114) exhibited a diffuse solvent ring at 3.3 Å. When allowed to dry, the sample showed a prominent sharp ring at 4.73 Å, consistent with the spacing between neighboring H-bonded polypeptide chains in a cross-β configuration. An identical diffraction pattern was obtained from peptide PrP-(127–147) (Fig. 3*d*). The ring with 4.73 Å spacing was weak when the peptide was in the form of a lyophilized powder and became sharp and strong after suspension of peptide in 30% formic acid.

DISCUSSION

The conversion of PrP^{C} to PrP^{Sc} is the molecular signature of prion-related encephalopathies (6). Limited proteolysis of PrP^{Sc} leads to release of a protease-resistant core that aggregates into amyloid fibrils (7–11). The present study shows that PrP peptides homologous to residues 106–126 and 127–147 readily assemble into fibrils that exhibit morphological, tinctorial, optical, and conformational properties of native amyloid. These peptides are included in the C-terminal half of the 11-kDa amyloid protein purified from GSS-Ik (20) and are located in the N-terminal region of PrP 27-30 (10), suggesting that the PrP sequence extending from residue 106 to residue 147 may be central for amyloidogenesis in prion-related encephalopathies. Ultrastructural and x-ray diffraction analysis extend recent observations reported by Gasset *et al.* (26) that peptides homologous to residues 109–122, 113–127, and 113–120 of Syrian hamster PrP form amyloid fibrils *in vitro* and exhibit a secondary structure composed largely of β-sheets, as assessed by attenuated total reflection Fourier transform infrared spectroscopy. However, whereas these investigators attributed fibril formation to the alanine-rich sequence AGAAAAGA (26), our data show that other sequences are also amyloidogenic, albeit with differing morphology and diffraction patterns. Within the PrP region spanning amino acids 106–147, residue 117 is a site of mutation (Ala → Val) genetically linked to GSS (27), and residue 129 corresponds to a polymorphism (Met → Val) that is associated with the phenotypic expression of clinically and pathologically distinct encephalopathies (i.e., Creutzfeldt–Jakob disease and fatal familial insomnia) linked to the same mutation (GAC → AAC, Asp → Asn) at PrP codon 178 (28). Whether such amino acid substitutions have significant effects on fibrillogenesis of PrP peptides remains to be established.

The observation that biochemically distinct inherited amyloidoses segregate with mutations of the gene encoding the amyloid protein precursor (29) has raised the issue as to how such differences in primary sequence might influence amyloid formation. Since synthetic peptides PrP-(169–185) and Prp-(195–213) that carry the codon 178 or codon 200 mutation genetically linked to familial Creutzfeldt–Jakob disease are more fibrillogenic than their normal homologues, it has been suggested that amino acid changes may alter the folding pattern of PrP to produce a β-pleated configuration (30). With respect to the PrP mutation linked to GSS-Ik, we found that peptides PrP-(191–205) and -(181–205) do not possess the intrinsic ability to assemble into amyloid-like fibrils, regardless of the presence of the mutant Ser-198. This finding is consistent with the previous observation that the PrP region containing the mutation is not present in peptides purified from GSS-Ik amyloid deposits (20) and suggests that the codon 198 mutation is not required for the adoption of a fibrillar configuration *in vitro*. It remains possible, however, that the mutation may exert a facilitatory role in promoting amyloidogenesis in affected patients, perhaps by exposing parts of the subsequence, residues 106–147 of PrP or by any other long-distance tertiary interactions. Thus, GSS-Ik differs from other amyloidoses such as hereditary cerebral amyloid angiopathy Dutch type and familial amyloidosis Finnish type, in which a point mutation in the gene encoding the precursor protein is expressed as an amino acid substitution in the amyloid protein (31–34), and this change enhances the rate of polymerization of synthetic peptide analogues *in vitro* (35, 36) and increases fibril stability (37).

Peptides PrP-(106–126) and PrP-(127–147) formed polymorphic structures that were distinct ultrastructurally. PrP-(106–126) fibrils resembled those extracted from amyloid deposits of GSS patients (20). It is likely that the major determinants of fibril morphology are contained in the polar

N-terminal stretch of this peptide rather than in the hydrophobic C-terminal region, since PrP-(106–114) fibrils were ultrastructurally similar to those obtained with PrP-(106–126), whereas PrP-(113–126) fibrils were reduced both in length and diameter. On the other hand, fibrils formed by PrP-(127–147) were distinct in being helically wound around each other with a well-defined periodicity. The generation of such fibrillar aggregates requires that PrP-(127–147) be intact, since shorter peptides PrP-(127–135) and PrP-(135–147) as well as peptides homologous to residues 129–140 of Syrian hamster PrP (26) and residues 119–138 of human PrP (30) are nonfibrillogenic. The inherent tendency of PrP-(127–147) to form twisted fibrillary structures suggests the possibility that this subsequence may be responsible for the morphology of scrapie-associated fibrils extracted from brains of humans and animals with transmissible spongiform encephalopathies, which are composed of a pair of short (4- to 6-nm diameter) filaments wrapped around each other with a pitch of 40–80 nm (38, 39).

X-ray diffraction analysis of fibrils formed by peptides PrP-(106–126), PrP-(106–114), and PrP-(127–147) resembles the characteristic pattern initially described for amyloid fibrils isolated from cases of AA and AL amyloidosis (40). This 4.7-Å/10-Å periodicity has also been found for amyloid fibrils extracted from the brains of Alzheimer patients (41) and for fibrillogenic peptides homologous to portions of the β-protein (25, 42, 43). Similar spacing was obtained for a synthetic peptide corresponding to a segment of the pancreatic islet amyloid protein (44). In addition to diffuse rings at 4.48 Å and 3.75 Å, the diffraction analysis of peptide PrP-(106–126) revealed reflections at 5.60–7.45 Å and 10.50–20.10 Å. Further studies of better oriented specimens should identify wide-angle reflections that may be due to intermolecular lateral packing of sheets, periodic fluctuations along the fiber axis (e.g., twisting of fibrils), or interposition of parts of the peptide between β-sheet in the fibril.

Our findings provide a basis for further studies aiming to elucidate the molecular mechanisms involved in PrP amyloid formation. In the present investigation, the most highly fibrillogenic peptide corresponded to residues 106–126 of PrP. It has been found recently that the chronic application of this peptide to rat hyppocampal cultures causes neuronal death by apoptosis (45). If PrP amyloid peptides formed *in vivo* confirm this neurotoxic effect, this would indicate that amyloidogenesis plays a key role in the pathogenesis of GSS and related encephalopathies.

This work was supported in part by the Italian Ministry of Health, Department of Social Services, and by the U.S. Public Health Service (Grants NS29822 to B.G. and NS30455 to B.F.).

1. Oesch, B., Westaway, D., Wälchli, M., McKinley, M. P., Kent, S. B. H., Aebersold, R., Barry, R. A., Tempst, P., Teplow, D. B., Hood, L. E., Prusiner, S. B. & Weissmann, C. (1985) *Cell* **40,** 735–746.
2. Chesebro, B., Race, R., Wehrly, K., Nishio, J., Bloom, M., Lechner, D., Bergstrom, S., Robbins, K., Mayer, L., Keith, J. M., Garon, C. & Haase, A. (1985) *Nature (London)* **315,** 331–333.
3. Kretzschmar, H. A., Prusiner, S. B., Stowring, L. E. & DeArmond, S. J. (1986) *Am. J. Pathol.* **122,** 1–5.
4. Stahl, N., Borchelt, D. R., Hsiao, K. & Prusiner, S. B. (1987) *Cell* **51,** 229–240.
5. Tagliavini, F., Prelli, F., Porro, M., Salmona, M., Bugiani, O. & Frangione, B. (1992) *Biochem. Biophys. Res. Commun.* **184,** 1398–1404.
6. Prusiner, S. B. (1992) *Biochemistry* **49,** 12277–12288.
7. Bolton, D. C., McKinley, M. P. & Prusiner, S. B. (1982) *Science* **218,** 1309–1311.
8. Prusiner, S. B., Bolton, D. C., Grooth, D. F., Bowman, K. A., Cochran, S. P. & McKinley, M. P. (1982) *Biochemistry* **21,** 6942–6950.
9. McKinley, M. P., Bolton, D. C. & Prusiner, S. B. (1983) *Cell* **35,** 57–62.
10. Prusiner, S. B., Grooth, D. F., Bolton, D. C., Kent, S. B. & Hood, L. E. (1984) *Cell* **38,** 127–134.
11. Prusiner, S. B., McKinley, M. P., Bowman, K. A., Bolton, D. C., Bendheim, P. E., Grooth, D. F. & Glenner, G. G. (1983) *Cell* **35,** 349–358.
12. Gasset, M., Baldwin, M. A., Fletterick, R. J. & Prusiner, S. B. (1993) *Proc. Natl. Acad. Sci. USA* **90,** 1–5.
13. Gerstmann, J., Sträussler, E. & Scheinker, I. (1936) *Z. Gesamte Neurol. Psychiatr.* **154,** 736–762.
14. Farlow, M. R., Tagliavini, F., Bugiani, O. & Ghetti, B. (1991) in *Handbook of Clinical Neurology: Hereditary Neuropathies and Spinocerebellar Atrophies*, ed. de Jong, J. M. B. V. (Elsevier, Amsterdam), Vol. 60, pp. 619–633.
15. Hsiao, K., Dlouhy, S., Farlow, M., Cass, C., DaCosta, M., Conneally, P. M., Hodes, M. E., Ghetti, B. & Prusiner, S. B. (1992) *Nat. Genet.* **1,** 68–71.
16. Dlouhy, S. R., Hsiao, K., Farlow, M. R., Foroud, T., Conneally, P. M., Johnson, P., Prusiner, S. B., Hodes, M. E. & Ghetti, B. (1992) *Nat. Genet.* **1,** 64–67.
17. Ghetti, B., Tagliavini, F., Masters, C. L., Beyreuther, K., Giaccone, G., Verga, L., Farlow, M. R., Conneally, P. M., Dlouhy, S. R., Azzarelli, B. & Bugiani, O. (1989) *Neurology* **39,** 1453–1461.
18. Giaccone, G., Tagliavini, F., Verga, L., Frangione, B., Farlow, M. R., Bugiani, O. & Ghetti, B. (1990) *Brain Res.* **530,** 325–329.
19. Tagliavini, F., Giaccone, G., Prelli, F., Verga, L., Porro, M., Trojanowski, J. Q., Farlow, M. R., Frangione, B., Ghetti, B. & Bugiani, O. (1993) *Brain Res.* **616,** 325–328.
20. Tagliavini, F., Prelli, F., Ghiso, J., Bugiani, O., Serban, D., Prusiner, S. B., Farlow, M. R., Ghetti, B. & Frangione, B. (1991) *EMBO J.* **10,** 513–519.
21. Giaccone, G., Verga, L., Bugiani, O., Frangione, B., Serban, D., Prusiner, S. B., Farlow, M. R., Ghetti, B. & Tagliavini, F. (1992) *Proc. Natl. Acad. Sci. USA* **89,** 9349–9353.
22. Garnier, J., Osguthorpe, D. J. & Robson, B. (1978) *J. Mol. Biol.* **120,** 97–120.
23. Eisenberg, D., Schwarz, E., Komaromy, M. & Wall, R. (1984) *J. Mol. Biol.* **179,** 125–142.
24. Chou, P. Y. & Fasman, G. D. (1978) *Annu. Rev. Biochem.* **47,** 251–276.
25. Gorevic, P. D., Castaño, E. M., Sarma, R. & Frangione, B. (1987) *Biochem. Biophys. Res. Commun.* **147,** 854–862.
26. Gasset, M., Baldwin, M. A., Lloyd, D. H., Gabriel, J. M., Holtzman, D. M., Cohen, F., Fletterick, R. & Prusiner, S. B. (1992) *Proc. Natl. Acad. Sci. USA* **89,** 10940–10944.
27. Doh-ura, K., Tateishi, J., Sasaki, H., Kitamoto, T. & Sakaki, Y. (1989) *Biochem. Biophys. Res. Commun.* **163,** 974–979.
28. Goldfarb, L. G., Petersen, R. B., Tabaton, M., Brown, P., LeBlanc, A. C., Montagna, P., Cortelli, P., Julien, J., Vital, C., Pendelbury, W. W., Haltia, M., Willis, P. R., Hauw, J. J., McKeever, P. E., Monari, L., Schrank, B., Swergold, G. D., Autilio-Gambetti, L., Gajdusek, D. C., Lugaresi, E. & Gambetti, P. (1992) *Science* **258,** 806–808.
29. Castaño, E. M., Wisniewski, T. & Frangione, B. (1991) *Curr. Opinion Neurobiol.* **1,** 448–454.
30. Goldfarb, L. G., Brown, P., Haltia, M., Ghiso, J., Frangione, B. & Gajdusek, D. C. (1993) *Proc. Natl. Acad. Sci. USA* **90,** 4451–4454.
31. Levy, E., Carman, M. D., Fernandez-Madrid, I., Lieberburg, I., Power, M. D., Van Duinen, S. G., Bots, G. T. A. M., Luyendijk, W. & Frangione, B. (1990) *Science* **248,** 1124–1126.
32. Prelli, F., Levy, E., Van Duinen, S. G., Bots, G. T. A. M., Luyendijk, W. & Frangione, B. (1990) *Biochem. Biophys. Res. Commun.* **170,** 301–307.
33. Levy, E., Haltia, M., Fernandez-Madrid, I., Koivunen, O., Ghiso, J., Prelli, F. & Frangione, B. (1990) *J. Exp. Med.* **172,** 1865–1867.
34. Maury, C. P. J. (1991) *J. Clin. Invest.* **87,** 1195–1199.
35. Wisniewski, T., Ghiso, J. & Frangione, B. (1991) *Biochem. Biophys. Res. Commun.* **179,** 1247–1254.
36. Maury, C. P. J. & Nurmiaho-Lassila, E.-L. (1992) *Biochem. Biophys. Res. Commun.* **183,** 227–231.
37. Fraser, P. E., Nguyen, J. T., Inouye, H., Surewicz, W. K., Selkoe, D. J., Podlisny, M. B. & Kirschner, D. A. (1992) *Biochemistry* **31,** 10716–10723.
38. Diringer, H., Gelderblom, H., Hilmert, H., Ozel, M., Edelbluth, C. & Kimberlin, H. (1983) *Nature (London)* **306,** 476–478.
39. Merz, P. A., Rohwer, R. G., Kascsak, R., Wisniewski, H. M., Somerville, R. A., Gibbs, C. J., Jr., & Gajdusek, D. C. (1984) *Science* **225,** 437–440.
40. Glenner, G. G., Eanes, E. D., Bladen, H. A., Linke, R. P. & Termine, J. D. (1974) *J. Histochem. Cytochem.* **22,** 1141–1158.
41. Kirschner, D. A., Abraham, C. & Selkoe, D. J. (1986) *Proc. Natl. Acad. Sci. USA* **83,** 503–507.
42. Kirschner, D. A., Inouye, H., Duffy, L. K., Sinclair, A., Lind, M. & Selkoe, D. J. (1987) *Proc. Natl. Acad. Sci. USA* **84,** 6953–6957.
43. Fraser, P. E., Nguyen, J. T., Surewicz, W. T. & Kirschner, D. A. (1991) *Biophys. J.* **60,** 1190–1201.
44. Glenner, G. G., Eanes, E. D. & Wiley, C. A. (1988) *Biochem. Biophys. Res. Commun.* **155,** 608–614.
45. Forloni, G., Angeretti, N., Chiesa, R., Monzani, E., Salmona, M., Bugiani, O. & Tagliavini, F. (1993) *Nature (London)* **362,** 543–545.